JOURNAL OF SPACECRAFT AND ROCKETS
Vol. 30, No. 6, November–December 1993

Comparison of Missile Flight-Test Drag with Aerodynamic Predictions

Donald W. Eastman*
The Boeing Company, Seattle, Washington 98124

Drag data from flight tests of a slender missile are compared with predictions at Mach numbers from 0.9 to 2.9, for angles of attack from 0 to 18 deg. Flight-test data for unpowered flight compares well with predictions at transonic speeds and is about 5% less than predictions at supersonic speeds. Methods used to predict drag and reasons for differences between the flight test and predicted drag are discussed.

Nomenclature

A_{ref} = reference area, 1.485 ft^2
A_{wet} = wetted area, ft^2
C_A = axial force coefficient
C_P = pressure coefficient
h = altitude, ft
L = length for Reynolds number (full scale), 20.0 ft for body, 0.83 ft for tail fins
M = freestream Mach number
Re = Reynolds number based on length L
Re/L = Reynolds number per ft
α = angle of attack, deg
δ_E = tail elevator angle, deg
$\delta_{elevator}$ = tail elevator angle, deg

Introduction

CURRENT drag prediction methods for air vehicles are based on a combination of scale model test data, analysis, and semi-empirical data. Recently, two flight tests of a missile were completed, which provide data for evaluating these methods. The missile, shown in Figs. 1 and 2, had four controlled wrap-around tail fins and an integral solid propellant booster. References 1 and 2 are earlier papers that present data on the evolving missile configuration.

Data presented here are in the body axis system, so that the term axial force instead of drag should properly be used. However, since these words are often interchanged, we often refer to drag instead of axial force.

Flight-Test Data

The two flight-test vehicles were designated FTV-1 and FTV-2. Each vehicle was boosted to approximately Mach 3.0 and then decelerated along the trajectories shown in Fig. 3. The FTVs flew at a constant heading, so that maneuvers in the lateral direction were minimal. Tails were in the X position, and all four fins were deflected together to control pitch, yaw, and roll.

Sounding balloons were launched about 30 min before each flight to measure atmospheric properties. Air properties coincided with the U.S. Standard Atmosphere. Wind measurements are shown in Fig. 4.

Atmospheric properties, weights, and onboard inertial measurement unit data, substantiated by ground tracking, were used to calculate the drag coefficients shown in Figs. 5–7. When these coefficients were input for six-degree-of-freedom trajectory simulations, the simulations closely matched the flight-test trajectories. This indicated that the drag data were compatible with the measured trajectories.

Drag measurements for the two flights were consistent as shown in Figs. 5–7. These flights had different trajectories with one into a head wind and the other into a tail wind. Drag data near Mach 2.0, which were measured over a wide range of altitude and wind conditions, had little scatter as shown in Fig. 5. Therefore, confidence in the accuracy of the FTV drag data was good.

Wind-Tunnel Tests

Tests were conducted on a 1/6 scale model of the configuration shown in Fig. 1 in the CALSPAN Transonic and the LTV high-speed wind tunnels, at the conditions shown in Table 1.

The model was sting mounted, except for the base drag model discussed later. Boundary-layer trips were installed on the body, 1 in. from the nose, and on each tail fin, 0.5 in. from the leading edge. The body was smooth and did not have the excrescences or raceway shown in Fig. 2.

The maximum drag measurement error of the balance was 1.3% at supersonic speeds, whereas the maximum error in test section dynamic pressure was 1%. Accuracy of the drag measurements, except base drag, was partially substantiated by comparing them with measurements on earlier models. For example, results from Ref. 1, when adjusted for configuration and test condition differences, were consistent with the data presented here. Also body-alone measurements compared well with analytical predictions at supersonic speeds as shown in Fig. 8.

Drag Prediction Methods

Because predicted drag is obtained by adding several drag components, a knowledge of each component is necessary to evaluate the prediction methods.

Body-Alone Drag

For body-alone wind-tunnel tests and analyses, the cylindrical body was extended to the base of the model to simulate the tail fins being folded. Pressure drag on the body at supersonic speeds was predicted using a method of characteristics computer program (MOCHA). This program numerically solves the exact inviscid equations of motion, and its accuracy has been validated by comparison with experimental data. The subsonic flow region around the hemispherical nose was calculated using an inverse method computer program.

Completely turbulent flow was assumed to occur on the 1/6 scale body due to boundary-layer trips and on the FTVs due to the excrescences near the nose. A turbulent boundary-layer program, which is coupled with MOCHA, was used to calculate skin friction drag at supersonic speeds. The method of Spalding and Chi,[3] which assumes a flat plate without pressure and wall temperature

Received Nov. 9, 1991; presented as Paper 92-0076 at the AIAA 30th Aerospace Sciences Meeting, Reno, NV, Jan. 6–9, 1992; revision received June 8, 1992; accepted for publication Sept. 18, 1992.

*Senior Principal Engineer, Boeing Defense and Space Group. Member AIAA.

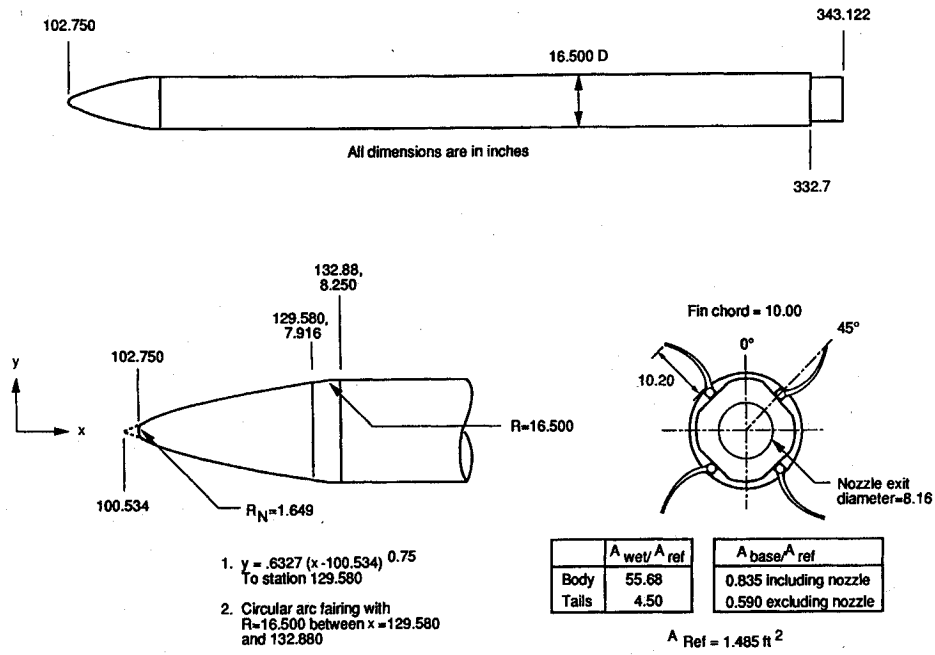

Fig. 1 Missile geometry.

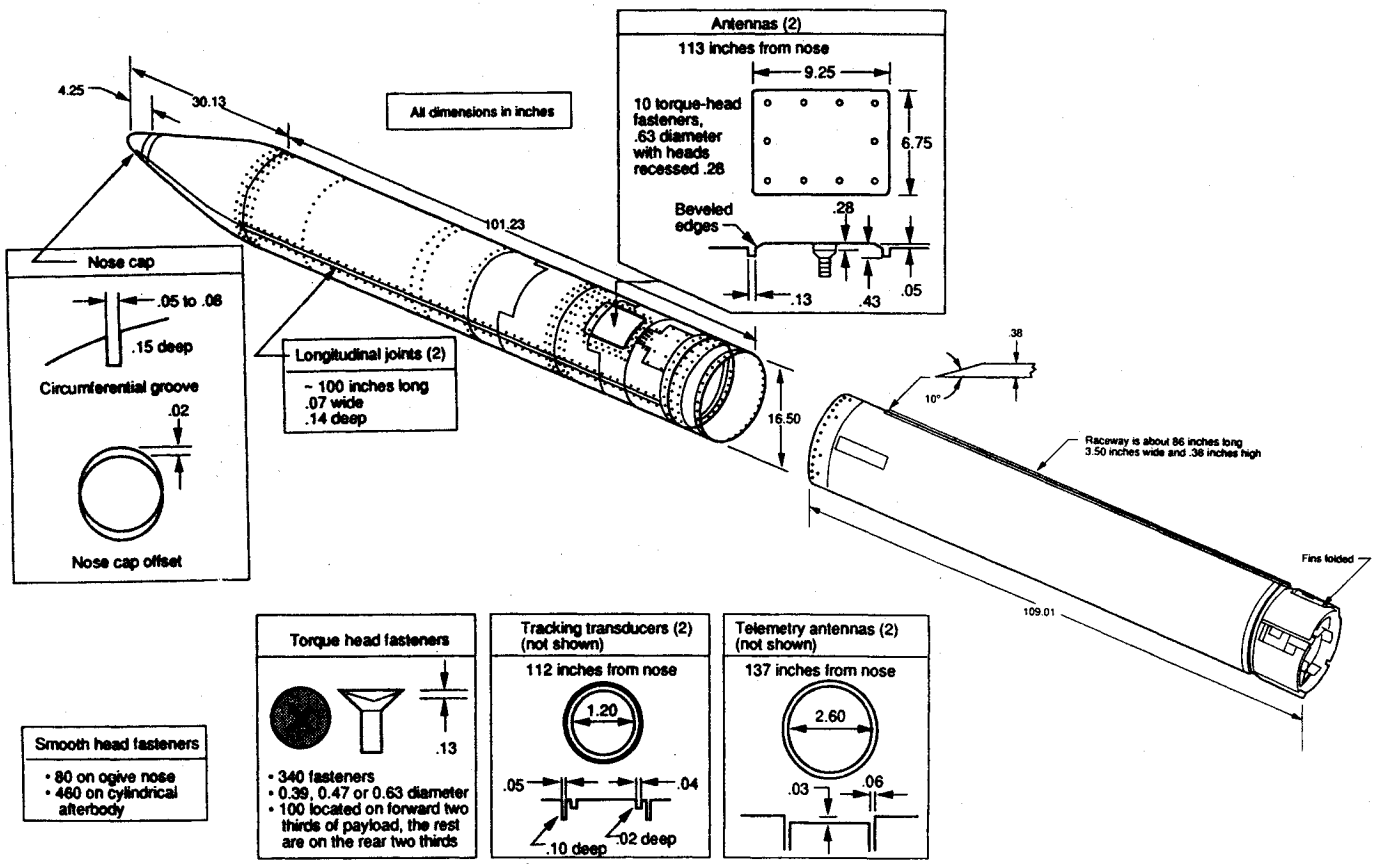

Fig. 2 FTV excrescences.

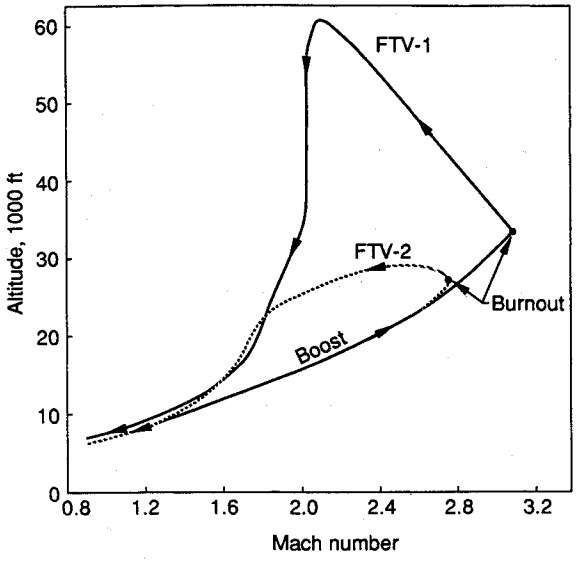

Fig. 3 FTV trajectories.

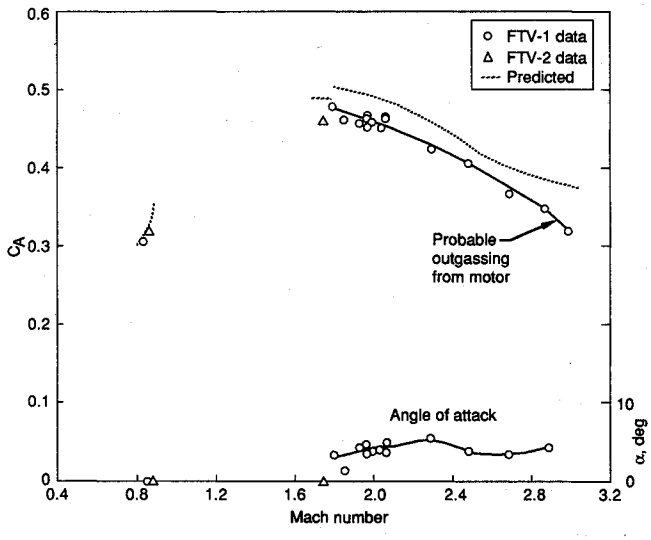

Fig. 5 Comparison of FTV and predicted axial force at small angles of attack.

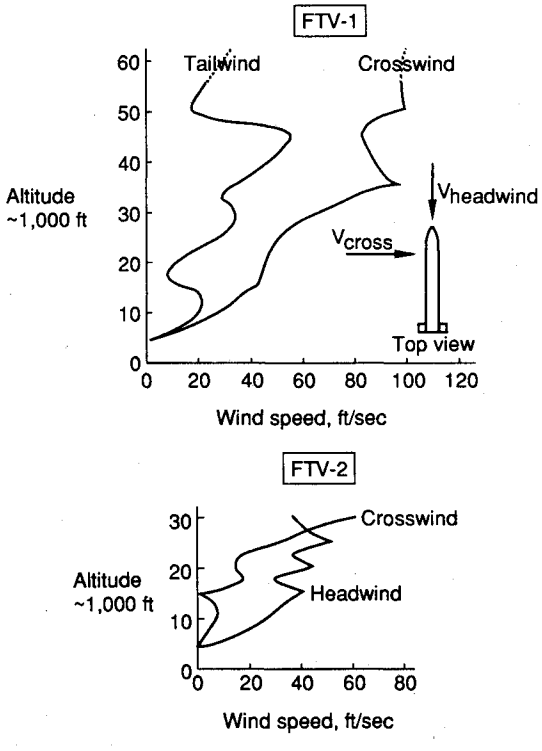

Fig. 4 Wind-speed measurements.

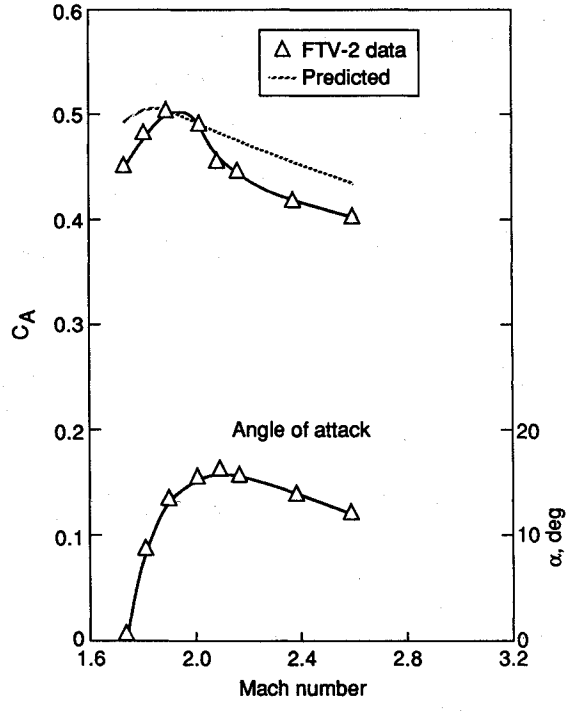

Fig. 6 Comparison of FTV-2 and predicted axial force.

gradients, was used to calculate local skin friction. An insulated wall was assumed for all calculations. These skin friction data were compared with flat plate drag calculated using the following Prandtl-Schlichting equation:

$$C_{D_F} = 0.455\,(A_{\text{wet}}/A_{\text{ref}})\,\frac{(1+0.144M^2)^{-0.65}}{(\log_{10}Re)^{2.58}} \qquad (1)$$

Because the two results were nearly equal, Eq. (1) was used to predict turbulent skin friction drag. The sum of pressure drag from MOCHA and skin friction drag from this equation compare well with wind tunnel data as shown in Fig. 8.

FTV pressure drag at transonic speeds was predicted by subtracting skin friction drag, calculated using Eq. (1), from the 1/6 scale model drag shown in Fig. 8. Skin friction drag for the FTVs was calculated using Eq. (1) and the Reynolds numbers for the trajectories shown in Fig. 3.

Tail Installation Drag

After testing the 1/6 scale body alone, the fairing that simulated the folded tail fins was removed and the four tail fins were installed to obtain the tail installation drag shown in Fig. 9. The drag difference between this configuration and the body alone represents the sum of 1) drag on the fins, 2) base drag on the body step just ahead of the fins, and 3) changes in body drag aft of the step.

Base pressure on the step was measured on the 1/6 scale model with the fins removed and used to calculate the step base drag shown in Fig. 9. Data by Tanner[4] indicate that the difference between wind-tunnel and FTV Reynolds numbers has a negligible

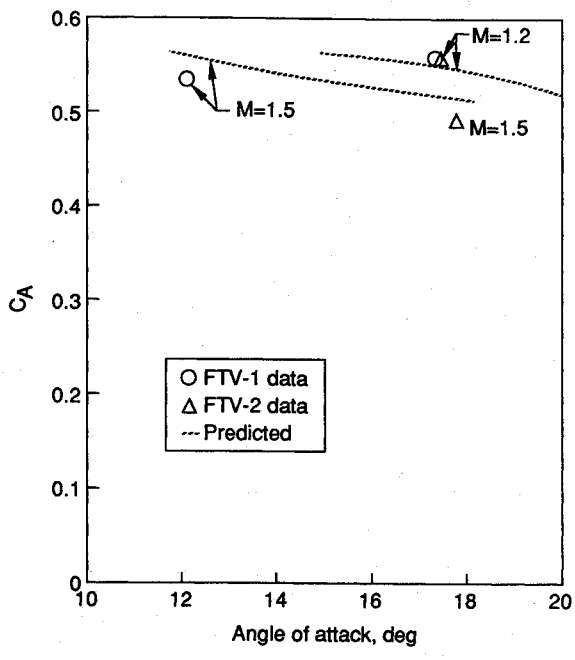

Fig. 7 Comparison of FTV and predicted axial force at large angles of attack.

effect on this pressure. Therefore, the same step drag increment was assumed to act on the FTVs.

Boundary-layer trips installed on the 1/6 scale model tail fins at 30% chord insured turbulent flow over 70% of the fin area. To be conservative, it was assumed that flow over the model fins was entirely turbulent. Fin skin friction drag, calculated using Eq. (1), is shown in Fig. 9.

For the FTVs it was assumed that flow on the tail fins was completely laminar, since their surface had a smooth finish and the fin Reynolds number was usually less than 5×10^6. Laminar skin friction drag was calculated using

$$C_{D_F} = 1.33\,(A_{\text{wet}}/A_{\text{ref}})/\sqrt{Re} \qquad (2)$$

Only adjustments to account for differences in skin friction drag were made to the tail installation drag shown in Fig. 9.

Excrescence Drag

Prediction of excrescence drag was approximate since 1) the prediction was made before the detailed excrescences were known, and 2) fabrication tolerances for the flight test vehicles were different from those of production vehicles. Excrescence drag was assumed to be 3% of the pressure and skin friction drag (excluding base drag) at 0-deg angle of attack. This value was consistent with that used on similar Boeing missiles.

Base Drag

The 1/6 scale model was strut mounted and tested in the LTV tunnel to measure base pressure.[2] Measurements at two supersonic speeds are shown in Fig. 10. Adjustments to base drag to account for differences between scale model and FTV Reynolds numbers were not made because Ref. 5 indicated that they were negligible.

Trim Drag

The axial force increment for trim shown in Fig. 11 was obtained from 1/6 scale model tests and accounts for changes in 1) body pressure and skin friction drag due to angle of attack, and 2) tail installation drag due to angle of attack and elevator angle. No adjustments were made to account for differences between model and FTV Reynolds numbers. (The effect of angle of attack and elevator angle on base drag was included in the base drag prediction.) Elevator angles required to trim are shown in Fig. 12. These angles, measured on the 1/6 scale model, compared well with FTV measurements.

Total Predicted Drag

Predicted drag components for FTV-1, at wind-tunnel test Mach numbers of 1.8 and 2.50, are tabulated in Fig. 13. Similar tabulations were used to develop the prediction curves in Figs. 5–7, where wind-tunnel data were faired between test Mach numbers.

Discussion of Results

Predicted drag was about 5% larger than flight-test data as shown in Figs. 5–7. Body pressure drag accounts for about 37% of the total drag at supersonic speeds, as shown in Fig. 13. Because this drag was calculated using the method of characteristics, the body pressure drag estimate is probably accurate. If so, the difference between the remaining predicted drag components and flight-test data is about 8% at supersonic speeds. Because of confidence in the accuracy of both the flight-test data and wind-tunnel measurements, this difference was not dismissed as being due to measurement error. Since several assumptions were made when adjusting wind-tunnel data to full-scale predictions, the impact of these assumptions on predicted drag was investigated.

Skin Friction Drag

Skin friction drag on the body accounts for about 20% of the total drag at supersonic speeds. Equation (1) was used to predict body skin friction drag because its results compared closely with those calculated using the method of Spalding and Chi. Their method, when compared with much experimental data, had a root-mean-square error of 10%,[3] which is equivalent to about 2% of the FTV drag. Although the method of Spaulding and Chi assumes that there is no pressure gradient, Wazzan and Ball[6] show that the effects of moderate pressure gradients on skin friction drag are small for turbulent flow.

When calculating skin friction drag, it was assumed that the boundary layer over the FTV body was completely turbulent. However, the favorable pressure gradient ($dp/dx<0$) along the nose may have delayed transition in spite of the excrescences shown in Fig. 2. If a transition Reynolds number of 10^7 is assumed, which is optimistic, drag is reduced about 1.5% at supersonic speeds.

Another source of error in skin friction calculations is related to wall temperature. Equation (1) is applicable when the boundary-layer recovery temperature is equal to the body wall temperature. This probably occurred on the forebody where the temperature of the thin aluminum shell quickly reacted to changes in recovery temperature. Conversely, the booster wall temperature increased after burnout because of heat transfer from within the booster. During static test firings, the wall temperature at burnout was about 580°R and increased at the rate of 0.7 deg/s. thereafter. Using these data, the predicted booster wall temperature for the FTVs varied from about 60 to 125% of the recovery temperature during supersonic flight. FTV drag would be reduced about 1% if the booster wall temperature was 125% of the recovery value.

Table 1 Test conditions for the 1/6 scale model

	Reynolds no./ft/10^6	
Mach no.	LTV	CALSPAN
0.6	5.3	3.9
0.9	6.6	2.9
1.05	—	2.5
1.09	7.1	—
1.2	—	2.4
1.33	7.6	—
1.8	6.4	—
2.5	7.5	—
4.0	13.5	—

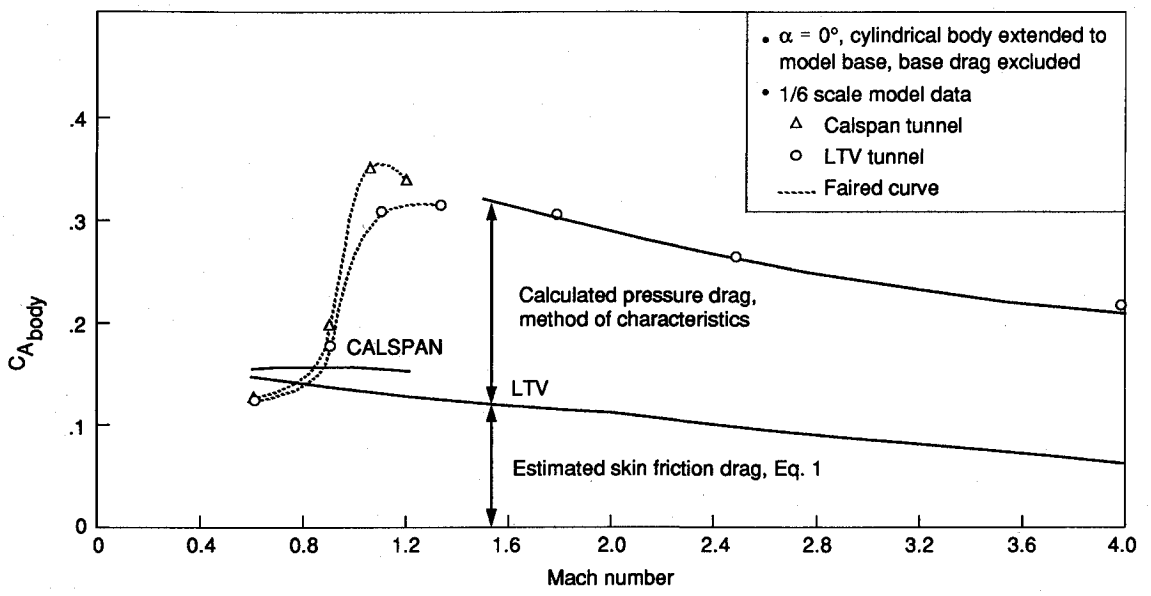

Fig. 8 Axial force on the 1/6 scale body-alone model.

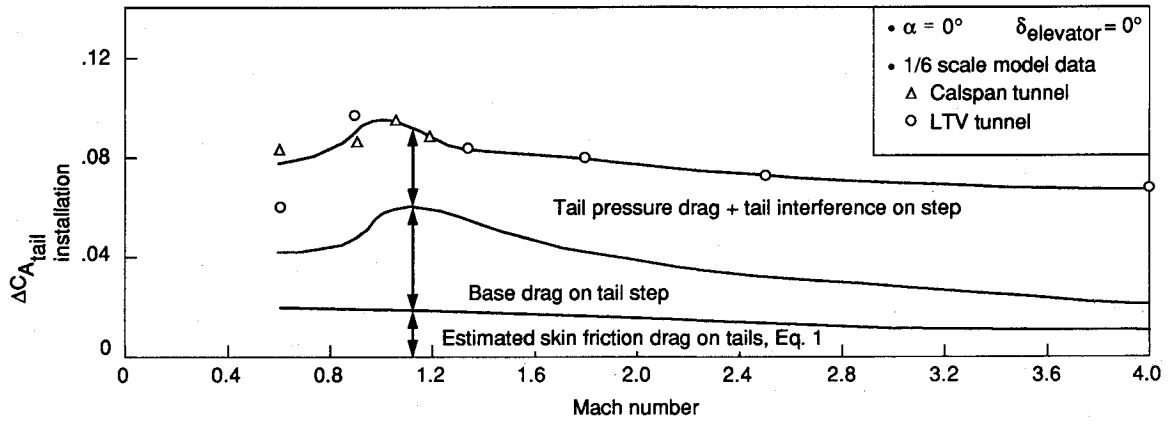

Fig. 9 Incremental axial force due to installing tails on the 1/6 scale model.

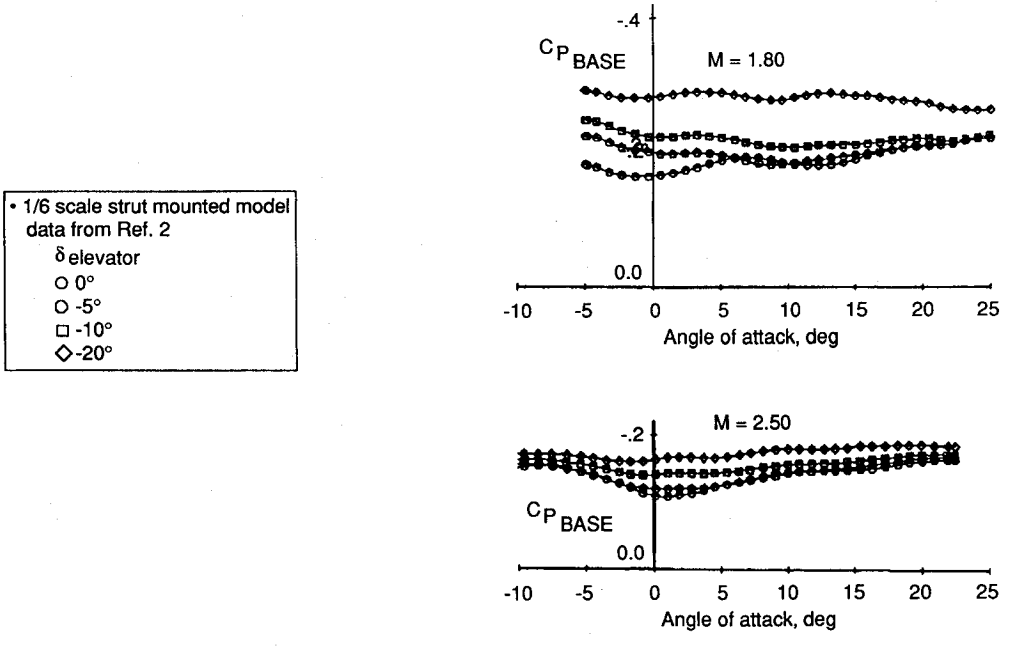

Fig. 10 Average base pressure on the 1/6 scale strut-mounted model.

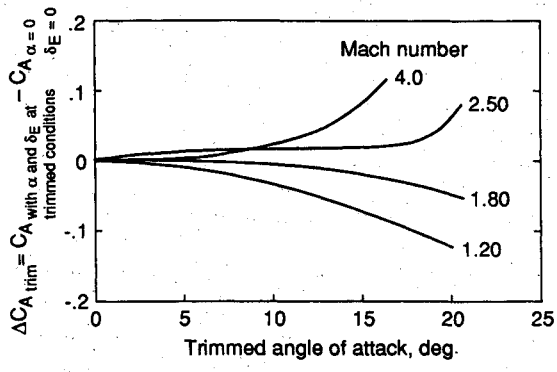

Fig. 11 Incremental axial force due to trim for the 1/6 scale model.

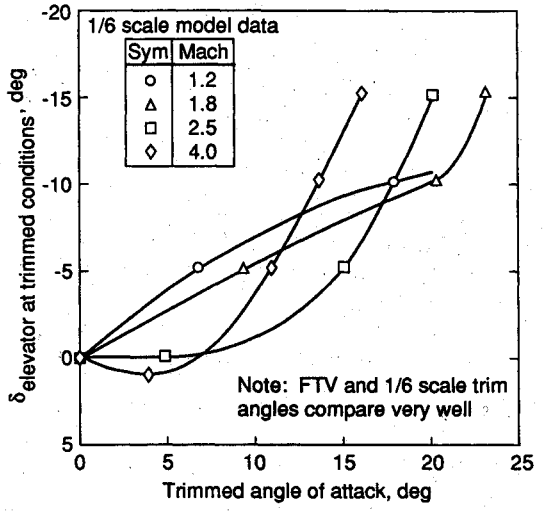

Fig. 12 Elevator angles at trimmed conditions for the 1/6 scale model.

Excrescence Drag

Although no firm basis exists for the 3% excrescence drag estimate, it was felt that this value was a reasonable estimate.

Base Drag

Base drag accounts for about 25% of the total drag at supersonic speeds. Wind-tunnel base pressure measurements in Fig. 10 agreed well with other experimental data,[2] yet a 20% error in these measurements could account for the difference between FTV and predicted drag. A pressure transducer was installed on each FTV to measure base pressure. Unfortunately, the electrical cables failed due to heating near the end of boost for both flights.

"Outgassing," which reduces base drag, occurs when motor insulation burns after the propellant is consumed. This probably caused the low drag near Mach 3.0 in Fig. 5, which was measured soon after motor burnout. Results in Ref. 7 indicate that outgassing at rates up to 0.21 lb/s would account for differences between predicted and FTV drag at Mach 1.8. This rate was possible for the FTV motor. However, to obtain the good correlation of FTV drag near Mach 2.0 in Fig. 5, outgassing would have needed to increase from 0.03 to 0.21 lb/s as time increased and altitude decreased.

The effect of flow differences on the FTV and scale model afterbodies was also considered. Pressure measurements on the step and base of the 1/6 scale model body are compared in Fig. 14. At Mach numbers of 1.8 and above, 1) the step pressure is equal to the base pressure, and 2) base pressure is not affected by removing the step. Therefore, the flows around the back of the model were probably merged into a single region as sketched in Fig. 15a. If the flow boundary on the FTVs moved closer to the body, as hypothesized in Fig. 15b, the resulting flow would be equivalent to that around a 4-deg conical boattail. The effect of boattail angle on drag of projectiles at Mach 1.70 is shown in Fig. 16.[8] Results indicate that if afterbody flow on the FTVs had formed a 4-deg quasiboat-tail angle, drag would have been reduced enough to account for the difference between flight-test data and predictions.

Component	Source of Data	Axial force coefficient		% of total predicted axial force	
		M = 1.80	M = 2.50	M = 1.80	M = 2.50
Body pressure drag ($\alpha = 0$)	Method of characteristics, Figure 8	.185	.161	37%	38%
Tail installation pressure drag ($\alpha = 0$)	Wind tunnel test, Figure 9	.061	.057	13%	14%
Skin friction drag h = 22,000 feet at M = 1.80 h = 51,000 feet at M = 2.50					
Body skin friction	Equation 1	.089	.084	18%	20%
Tail skin friction	Equation 2	.002	.004	< 1%	1%
Subtotal		.337	.306	—	—
3% of subtotal excrescence drag penalty	Estimate	.010	.009	2%	2%
Trim conditions $\alpha = 3°$, $\delta_E = -1.6$ at M = 1.80 $\alpha = 3.5°$, $\delta_E = 0$ at M = 2.50					
Base drag at trim conditions	Wind tunnel test, Figure 10	.153	.098	30%	23%
Trim drag	Wind tunnel test, Figure 11	0	.010	0%	2%
Total predicted axial force		.500	.423	100%	100%

Fig. 13 Predicted axial force for FTV-1 at Mach 1.8 and 2.5.

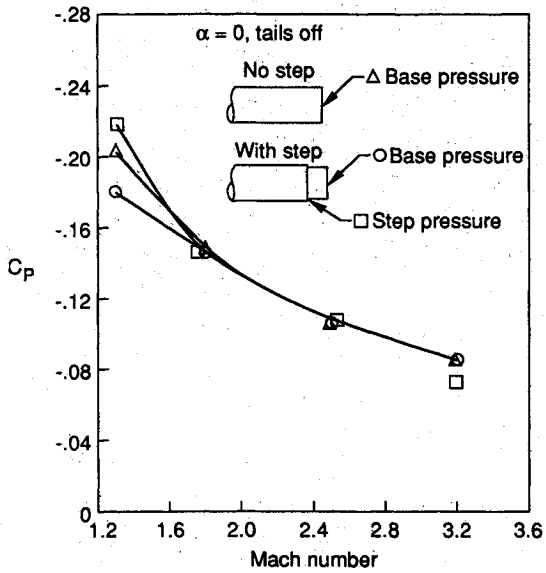

Fig. 14 Pressures on the base and step of the 1/6 scale sting-mounted model.

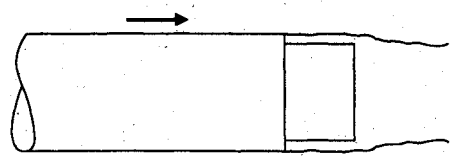

a) Flow behind step and in base region were merged into a single flow region on 1/6 scale model

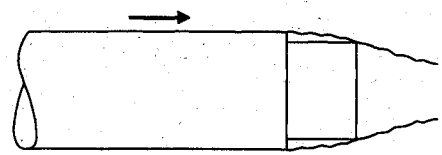

b) Flow behind step attached to body to form a quasi-boattail on FTVs

Fig. 15 Hypothesized afterbody flow regions.

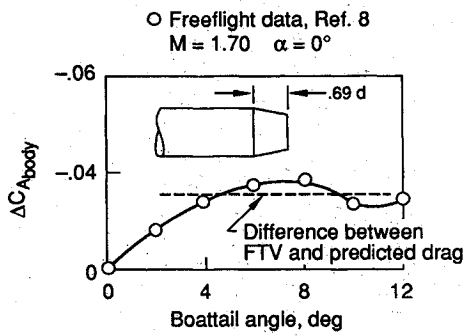

Fig. 16 Effect of boattail angle on body axial force.

Conclusions

Reasons that predicted drag at supersonic speeds was about 5% greater than flight-test measurements are unknown. Because of confidence in the accuracy of the flight-test and wind-tunnel data, it was not attributed to measurement error. Inaccuracies in methods used to predict skin friction and excrescence drag may have caused some of the difference. Also, wind-tunnel base pressure measurements may not have represented FTV base drag. Considering that base drag accounts for about 25% of the total drag, little is known about the combined effects of outgassing, angle of attack, fin deflection, geometry, and Reynolds number on this key drag component.

References

[1]Eastman, D. W., and Wenndt, D. L., "Aerodynamics of Maneuvering Missiles with Wrap-Around Fins," AIAA Paper 85-4083, Oct. 1985.

[2]Eastman, D. W., and Wenndt, D. L., "Base Drag of Highly Maneuvering Non-Thrusting Missiles," AIAA Paper 88-2544, June 1988.

[3]Spalding, D. B., and Chi, S. W., "The Drag of a Compressible Turbulent Boundary Layer on a Smooth Flat Plate With and Without Heat Transfer," *Journal of Fluid Mechanics*, Vol. B, Pt. 1, Jan. 1964, pp. 117–143.

[4]Tanner, M., "Boundary-Layer Thickness and Base Pressure," *AIAA Journal*, Vol. 23, No. 12, 1985, pp. 1987–1989.

[5]Tanner, M., "Steady Base Flow," *Progress in Aerospace Sciences*, Vol. 21, No. 2, 1984, pp. 81–157.

[6]Wazzan, A. R., and Ball, W. H., "Body Shape Effects on Skin Friction in Supersonic Flow," *AIAA Journal*, Vol. 3, No. 9, 1965, pp. 1770–1772.

[7]Danberg, J. E, and Nietubicz, C. J., "Predicted Flight Performance of Base-Bleed Projectiles," *Journal of Spacecraft and Rockets*, Vol. 29, No. 3, 1992, pp. 366–372.

[8]Karpov, B. G., "The Effect of Various Boattail Shapes on Base Pressure and Other Aerodynamic Characteristics on a 7-Caliber Body of Revolution at M=1.70," U.S. Army Ballistic Research Lab., BRL R 1295, Aberdeen Proving Ground, MD, Aug. 1965.

Gerald T. Chrusciel
Associate Editor